

Research paper

Kinetics and chemoselectivity studies of hydrogenation reactions of alkenes and alkynes catalyzed by (benzoimidazol-2-ylmethyl)amine palladium(II) complexes

Thandeka A. Tshabalala, Stephen O. Ojwach*

School of Chemistry and Physics, Pietermaritzburg Campus, University of KwaZulu-Natal, Private Bag X01, Scottsville 3209, South Africa

ARTICLE INFO

Keywords:

Palladium
Alkenes
Alkynes
Hydrogenation
Kinetics

ABSTRACT

A series of (benzoimidazol-2-ylmethyl)amine palladium(II) complexes have been employed as catalysts in the homogeneous hydrogenation of alkenes and alkynes under mild conditions. A correlation between the catalytic activity and the nature of the ligand was established. Kinetic studies of the hydrogenation reactions of styrene established *pseudo*-first-order dependence on styrene substrate. On the other hand, partial orders with respect to H₂ and catalyst concentrations were obtained. The nature of the solvent used influenced the hydrogenation reactions, where coordinating solvents resulted in lower catalytic activities. Kinetics and mechanistic studies performed were consistent with the formation of palladium monohydride intermediates as the active species.

1. Introduction

Hydrogenation reactions of alkenes and alkynes are currently one of the dominant industrial processes used for the reduction of unsaturated organic compounds to produce a wide range of relevant products [1–3]. Several metal-based catalysts derived from nickel, palladium, ruthenium, rhodium, iridium and platinum have been employed in the catalytic hydrogenation of alkenes and alkynes under both homogeneous [4,5] and heterogeneous [6,7] conditions. Currently, the major focus in transition metal catalyzed homogeneous molecular hydrogenation reactions has been on ligand design; and the insights gained so far show that the ability to control the catalytic behavior of these catalyst lies in the coordination environment around the metal atom.

In particular, palladium(II) catalysts are currently receiving much attention in the hydrogenation of alkenes and alkynes due to their superior catalytic activities and selectivity [8]. Numerous reports have appeared on the homogeneous hydrogenation of alkenes and alkynes using palladium(II) catalysts supported on phosphine-donor ligands. For example, Bacchi *et al* [9] and Drago *et al* [10] employed hydrazonic phosphine palladium(II) and bidentate (2,5-dimethylphospholano) palladium(II) complexes as effective catalysts in the hydrogenation of alkenes. Even though the phosphine-donor palladium(II) catalysts have been successfully used in the homogeneous hydrogenation reactions of alkenes and alkynes, these systems suffer from lack of stability and sensitivity to moisture and air [11]. As a result, nitrogen-donor

palladium(II) catalysts are emerging as suitable alternatives due to their better stability and ease of synthesis in comparison to the phosphine-donor palladium(II) complexes. For example, the pyridine-2-carbaldine palladium(0) [12] and bis(arylimino)acenaphthene palladium(0) [13] complexes have been shown to exhibit good selectivity and stability in the homogeneous hydrogenation of alkynes.

We recently reported the use of palladium(II) complexes anchored on (benzoimidazol-2-ylmethyl)amine ligands [14] to give active catalysts in the methoxycarbonylation of higher olefins. Due to the promising results obtained in the methoxycarbonylation reactions by these systems, we chose to explore their propensity to catalyze the molecular hydrogenation of selected alkenes and alkynes. In addition, detailed kinetics, mechanistic and theoretical studies have been performed and are herein discussed.

2. Experimental section

2.1. Materials and methods

All moisture and air sensitive reactions were performed using standard Schlenk line techniques. Methanol (ACS reagent, ≥99.8%), toluene (ACS reagent, ≥99.5%), dichloromethane (ACS reagent, ≥99.8%), absolute ethanol (ACS reagent, ≥98%) and tetrahydrofuran (anhydrous, ≥99.9%) were purchased from Merck. Solvents were dried and distilled under nitrogen in the presence of suitable drying agents:

* Corresponding author.

E-mail address: ojwach@ukzn.ac.za (S.O. Ojwach).

<https://doi.org/10.1016/j.ica.2018.08.004>

Received 22 May 2018; Received in revised form 7 August 2018; Accepted 7 August 2018

Available online 11 August 2018

0020-1693/ © 2018 Elsevier B.V. All rights reserved.

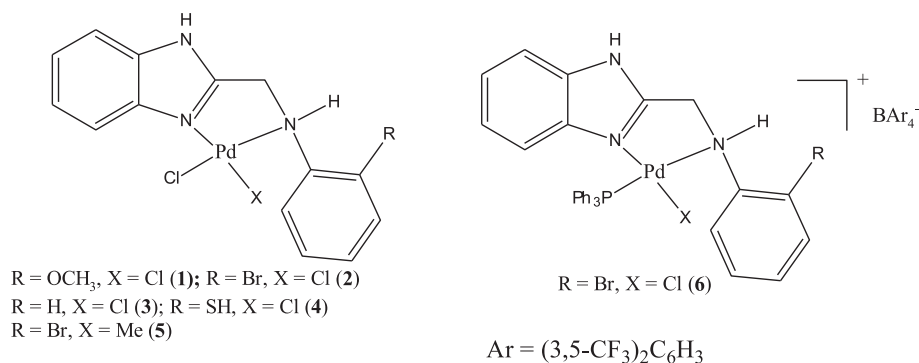


Fig. 1. Neutral and cationic (benzimidazol-2-ylmethyl)amine palladium (II) complexes 1–6 [14] used as catalysts in the hydrogenation reactions.

Toluene and acetone were dried over anhydrous calcium chloride, methanol and absolute ethanol over calcium oxide, dichloromethane over phosphorus pentoxide and stored over 4 Å molecular sieves. The ligands *N*-(1H-benzimidazol-2-ylmethyl-2-methoxy)aniline (**L1**), *N*-(1H-benzimidazol-2-ylmethyl-2-bromo)aniline (**L2**), *N*-(1H-benzimidazol-2-ylmethyl)benzenamine (**L3**) and *N*-(1H-benzimidazol-2-ylmethylamino)benzenethiol (**L4**), were synthesized following the published literature method [15]. The palladium complexes [Pd(**L1**)Cl₂] (**1**), [Pd(**L2**)Cl₂] (**2**), [Pd(**L3**)Cl₂] (**3**), [Pd(**L4**)Cl₂] (**4**), [Pd(**L2**)ClMe] (**5**) and [Pd(**L2**)ClPPh₃]⁺BAR₄[−] (**6**), were prepared following our recently published procedure [14].

2.2. Density Functional Theory (DFT) studies

DFT calculations were performed in a gas phase to identify the energy-minimized structures based on B3LYP/LANL2DZ (Los Alamos National Laboratory 2 double ζ) level theory [16]. A split bases set, LANL2DZ for palladium and 6-311G for all other atoms was used to optimize the geometries and energies of the complexes. The Gaussian09 suite of programs was used for all the computations.

2.3. General procedure for the hydrogenation reactions of alkenes and alkynes

The catalytic hydrogenation reactions were performed in a stainless steel autoclave equipped with temperature control unit and a sample valve. In a typical experiment, styrene (0.5 mL, 4.20 mmol) and complex **2** (3.47 mg, 0.007 mmol, S/C 600) were dissolved in toluene (50 mL). The reactor was evacuated, flushed with nitrogen and the catalytic solution was introduced to the reactor via a cannula. The reactor was purged three times with hydrogen, and then set at the equipped pressure, heated to the desired temperature and the reaction stirred at 500 rpm. At the end of the reaction time, the reactor was cooled, excess hydrogen vented off. Samples for GC analyses were drawn via a syringe, filtered using 0.45 μm micro filters and analyzed by Varian CP-3800 GC (ZB-5HT column 30 m \times 0.25 mm \times 0.10 μm) GC instrument to determine the percentage conversion of styrene to ethylbenzene. The percentage conversions were determined by comparing the peak areas of the alkene/alkyne substrate and respective products, assuming 100% mass balance. For example, comparison of peak areas of styrene and ethylbenzene at regular time intervals allowed the determination of the rate of conversion of styrene to ethylbenzene. Standard authentic samples; ethylbenzene (97%), *trans*-2-hexene (97%), *cis*-2-hexene (98%), *trans*-2-octene (98%) and octane (98%) were purchased from Sigma-Aldrich and used to confirm the presence and composition of hydrogenation products.

3. Results and discussion

3.1. Hydrogenation reactions of alkenes and alkynes using palladium (II) complexes 1–6 as catalysts

Preliminary evaluations of complexes 1–6 (Fig. 1) in the hydrogenation of styrene were performed at 5 bar of H₂ pressure, 30 °C and [styrene]/[catalysts] = 600:1. Under these conditions, all the complexes showed catalytic activities to afford 100% ethylbenzene with conversions ranging from 54% to 99% within 1.5 h (Fig. S1). In order to fully account for the role of complexes 1–6 in the observed catalytic hydrogenation reactions, control experiments were conducted without the use of the palladium(II) complexes and also in the presence of the ligand **L2** only under similar reaction conditions. The low percentage conversions of 4% and 6% obtained respectively within 10 h (Table 1, entries 7 and 8) confirmed that complexes 1–6 were responsible for the observed higher catalytic activities. We thus further carried out kinetics, selectivity, theoretical and mechanistic studies of hydrogenation reactions of alkenes and alkynes using complexes 1–6 as catalysts.

3.2. Kinetics of styrene hydrogenation reactions

3.2.1. Effect of complex structure on catalytic hydrogenation of styrene by 1–6

Kinetics of the hydrogenation reactions of styrene were investigated for complexes 1–6 by monitoring the reactions using GC chromatography. Table 1 contains the initial rate constants derived from the

Table 1
Effect of catalyst structure on the hydrogenation of styrene by complexes 1–6.^a

Entry	Catalyst	Conversion ^b (mol%)	k_{obs} (h ^{−1})	TOF ^c (h ^{−1})
1	1	74	0.91 (± 0.03)	296
2	2	92	1.67 (± 0.01)	368
3	3	78	0.98 (± 0.05)	312
4	4	86	1.38 (± 0.07)	344
5	5	54	0.56 (± 0.04)	215
6	6	99	2.93 (± 0.1)	396
7 ^d	—	4	—	—
8 ^e	—	6	—	—

^aConditions: styrene (0.41 g, 4.00 mmol); [styrene]/[catalyst], 600; substrate, catalyst (0.007 mmol); solvent, toluene (50 mL); pressure, 5 bar; temperature, 30 °C; time, 1.5 h.

^bDetermined by GC by comparing the peak areas of styrene substrate to ethylbenzene at regular time intervals.

^cTOF in mol_{substrate}mol_{catalyst}^{−1}h^{−1} (h^{−1}).

^dControl experiment, no catalyst used, time, 10 h.

^eControl experiment, in the presence of the ligand **L2**; time, 10 h.

Table 2Effect of catalyst concentration and pressure on the hydrogenation of styrene using catalysts **2** and **6**.^a

Entry	[sub]/[cat]	P_{H_2} (bar)	K_{obs} (h^{-1})		TOF (h^{-1}) ^b	
			2	6	2	6
1 ^c	200	5	3.84 (± 0.02)	6.32 (± 0.01)	158	198
2 ^d	400	5	2.66 (± 0.02)	3.56 (± 0.03)	267	316
3	600	5	1.67 (± 0.01)	2.92 (± 0.02)	368	396
4	800	5	1.45 (± 0.03)	1.79 (± 0.04)	448	501
5	1000	5	0.91 (± 0.05)	1.05 (± 0.05)	466	513
6	600	7.5	2.02 (± 0.02)	–	392	–
7 ^c	600	10	5.45 (± 0.13)	–	475	–
8 ^d	600	12.5	6.84 (± 0.06)	–	594	–
9 ^e	600	5	0.69 (± 0.03)	1.81 (± 0.03)	268	376

^aConditions: styrene, (4.00 mmol); solvent; toluene (50 mL); temperature, 30 °C; time, 1.5 h.^bTOF in $\text{mol}_{\text{substrate}}/\text{mol}_{\text{catalyst}} \text{ h}^{-1}$.^cTime, 1.0 h^dTime, 1.25 h.^eMercury drop test (5 drops of mercury were added to the reaction mixture).

plots of $\ln[\text{styrene}]_0/[\text{styrene}]_t$ vs time (Fig. S2). A linear relationship was established consistent with a *pseudo*-first order kinetics with respect to styrene for all the complexes. The dependence of the rate of the hydrogenation reactions on styrene substrate can therefore be represented as given in Eq. (1).

$$\text{Rate} = k[\text{styrene}]^1 \quad (1)$$

From the rate constants observed, the cationic complex **6** was the most active (Table 1, entries 2 and 6). This higher catalytic activity could be attributed to the improved solubility of complex **6** (due to the bulky Ar groups) compared to complexes **1–5** [11]. Another plausible explanation could be a higher positive charge on the palladium(II) metal atom in the cationic complex **6** relative to the neutral analogues, thus better substrate coordination [8]. A similar trend in the hydrogenation of 1-hexene was reported where higher catalytic activity ($\text{TOF} = 4000 \text{ h}^{-1}$) for the cationic complex $[\text{Rh}(\text{PPh}_3)_2\text{COD}]^+$ compared to $\text{TOF} = 700 \text{ h}^{-1}$ for the neutral complex $[\text{Rh}(\text{PPh}_3)_3\text{Cl}]$ was observed [17,18]. We also observed that the ligand motif had an influence on the catalytic activity. For instance, complex **2**, bearing electron withdrawing Br group on the phenyl ring showed higher catalytic activity, (k_{obs} of 1.67 h^{-1}) than the analogues complex **1** (k_{obs} of 0.91 h^{-1}), containing the electron donating OCH_3 substituent (Table 1, entries and 2). This can also be rationalized from electrophilic metal [8] center in **2** compared to **1**, consistent with the argument fronted for the

cationic complex **6**. Another factor that appeared to control the catalytic activity was the Pd-Cl/Me bonds on the complex structure. For example, rate constants of 1.67 h^{-1} and 0.56 h^{-1} were observed for complexes **2** and **5** bearing Pd-Cl and Pd-Me groups respectively (Table 1, entries 2 and 5). This can be attributed to enhanced stability of the dichloride complex **2**, compared to the Pd-Me complex **5**. Generally, metal alkyls are known to readily undergo deactivation due to the higher reactivity of metal-alkyl bonds [19].

3.2.2. Effect of catalyst concentration and hydrogen pressure on the kinetics of hydrogenation reactions of styrene

Kinetic experiments were further conducted to establish the effects of catalyst concentrations on the hydrogenation reactions of styrene using complexes **2** and **6**. The concentrations of catalysts **2** and **6** were thus varied from 200:1 to 1000:1 at constant initial concentration of styrene (Table 2, entries 1–5). Plots of $\ln[\text{styrene}]_0/[\text{styrene}]_t$ vs time (Fig. S3) gave linear relationships from which the observed rate constants (k_{obs}) were derived (Table 2). It was observed that an increase in catalyst concentration resulted in an increase in catalytic activity. For instance k_{obs} of 1.67 h^{-1} and 0.91 h^{-1} were obtained at $[\text{styrene}]/[\text{2}]$ ratios of 600 and 1000 respectively. However, a closer examination of the TOF values for both **2** and **6** at different catalyst loadings paint a different picture. For example, increased $[\text{styrene}]/[\text{6}]$ ratio (decrease in catalyst concentration) from 600 to 1000 was marked by an increase in TOF from 396 h^{-1} and 513 h^{-1} respectively (Table 2, entries 3–5). It is therefore evident that increasing catalyst concentration did not increase the catalytic activity by a similar magnitude and thus higher $[\text{substrate}]/[\text{catalyst}]$ ratios (lower catalyst loadings) is not only recommended but would also be industrially beneficial with these systems.

The orders of reaction with respect to catalysts **2** and **6** were extracted from the plots of $-\ln(k_{obs})$ vs $-\ln[\text{2}]$ and $-\ln[\text{6}]$ (Fig. 2) and obtained as 0.73 ± 0.08 and 1.03 ± 0.06 respectively (Eqs. 2 and 3). From our previous work, we reported fractional orders with respect to catalyst concentration in hydrogenation reactions of styrene catalyzed by palladium(II) complexes [20,21] and was associated with possible catalyst aggregation during the hydrogenation reactions and/or formation of palladium(0) nanoparticles as the active species [22,23]. On the other hand, the integer order with respect to the cationic complex **6** thus shows minimum aggregation of the active species, in good agreement with the value of 1.08 h^{-1} reported by Kluwer *et al.* [24]

$$\text{Rate} = k[\text{styrene}]^1 [\text{2}]^{0.73} \quad (2)$$

$$\text{Rate} = k[\text{styrene}]^1 [\text{6}]^{1.03} \quad (3)$$

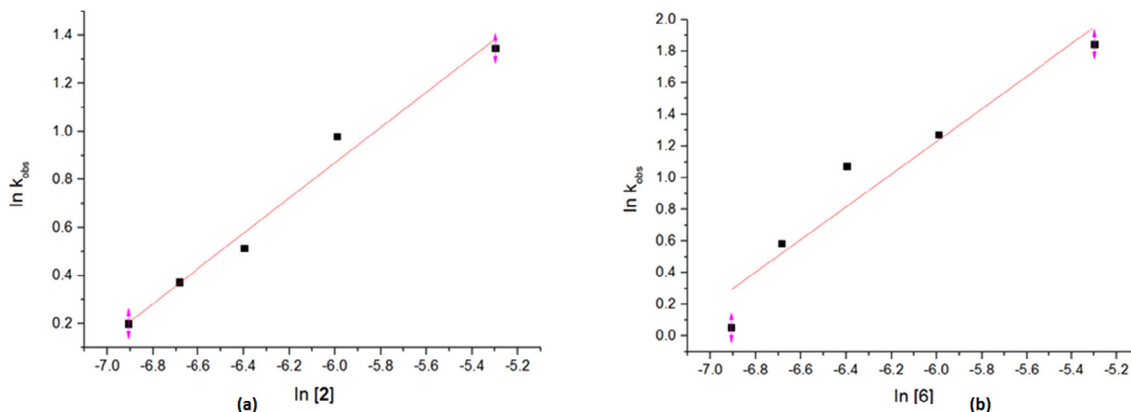


Fig. 2. Plot of $\ln(k_{obs})$ vs $\ln[\text{2}]$ (a) and $\ln[\text{6}]$ (b) for the determination of the order of reaction with respect to catalyst **2** and **6** in the hydrogenation of styrene. $R^2 = 0.98237$; slope = 0.73, Intercept = 5.56 (a) $R^2 = 0.96186$; slope = 1.03, Intercept = 7.41 (b).

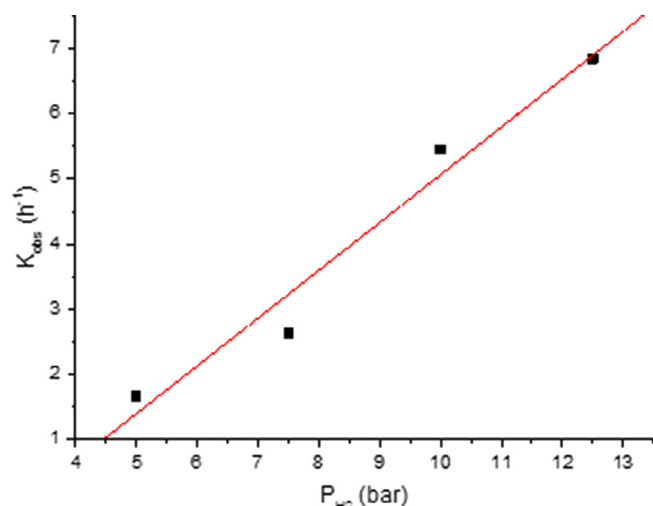


Fig. 3. Plot of k_{obs} vs P_{H_2} (bar) for the determination of the order of reaction with respect to H_2 pressure in the hydrogenation of styrene using catalyst 2. $R^2 = 0.98271$; slope = 0.73, Intercept = 2.26.

Table 3

Effect of temperature and solvent on the hydrogenation of styrene using catalyst 2.^a

Entry	Solvent	T (°C)	Conv (%) ^b	k_{obs} (h ⁻¹)	TOF (h ⁻¹) ^c
1	Toluene	30	92	1.67 (± 0.01)	368
2 ^d	Toluene	40	99	4.19 (± 0.03)	475
3 ^d	Toluene	50	> 99	5.46 (± 0.1)	480
4 ^e	Toluene	60	> 99	6.30 (± 0.07)	600
5	Methanol	30	49	0.61 (± 0.08)	196
6	DCM	30	68	0.90 (± 0.04)	272
7	THF	30	86	1.40 (± 0.03)	343
8	DMSO	30	35	0.52 (± 0.06)	183

^aConditions: styrene (0.41 g, 4.00 mmol); solvent; toluene (50 mL); [styrene]/[2] = 600; time, 1.5 h, pressure, 5 bar.

^bDetermined by GC by comparison of peak areas of styrene and ethylbenzene product.

^cTOF in mol_{substrate}mol_{catalyst}⁻¹ h⁻¹ (h⁻¹).

^dTime, 1.25 h

^eTime, 1.0 h.

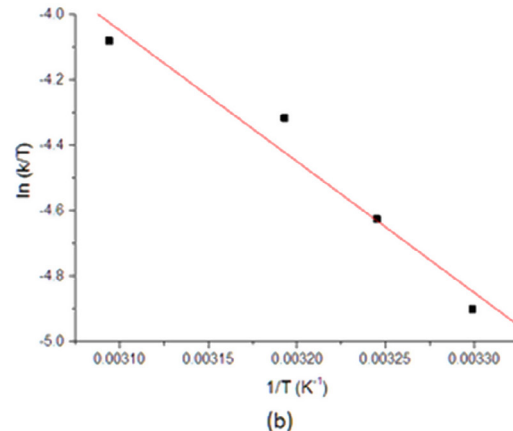
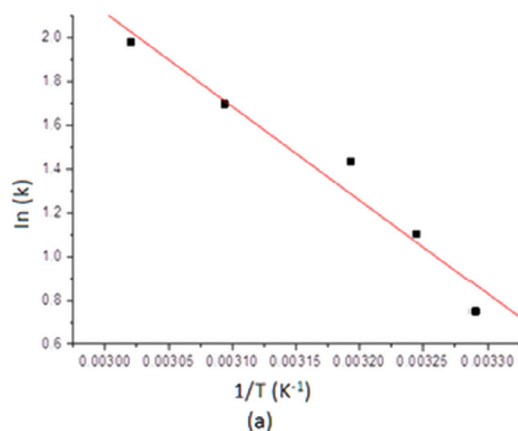


Fig. 4. Arrhenius plot (a) and Eyring plot (b) for the determination of the $E_a = 35.61 \pm 1.6 \text{ kJ mol}^{-1}$, $\Delta H^\ddagger = 32.98 \pm 1.9 \text{ kJ mol}^{-1}$, and $\Delta S^\ddagger = -127.9 \pm 1.9 \text{ J mol}^{-1} \text{ K}^{-1}$ for the hydrogenation of styrene using catalyst 2. $R^2 = 0.9645$; slope = -42823 ; Intercept = 553 (a), $R^2 = 0.9724$; slope = -4006 ; Intercept = 611 (b).

To shed some light on the possible formation of palladium(0) nanoparticles, mercury poisoning test was conducted for catalysts 2 and 6 by adding few drops of mercury to the reaction solutions [22]. While appreciable drop in catalytic activity from 92% ($k_{obs} = 1.67 \text{ h}^{-1}$) to 67% ($k_{obs} = 0.69 \text{ h}^{-1}$) was observed for catalyst 2, catalyst 6 exhibited minimal decline in catalytic activity from 99% ($k_{obs} = 2.92$) to 94% ($k_{obs} = 1.81$), (Table 2, entries 3 and 9). This showed possible formation of more nanoparticles in catalyst 2 compared to catalyst 6 [21] in good agreement with kinetic Eqs. (2) and (3). In general, the absence of induction periods (Figs. S1–S6) point to a largely homogeneous catalyst systems for both complexes 2 and 6.

The effect of H_2 concentration on the kinetics of styrene hydrogenation reactions was also investigated at different H_2 pressures of 5 bar to 12.5 bar (Table 2, entries 3, 6–8). From the data obtained, it was evident that an increase in H_2 pressure resulted in an increase in the observed rate constants (k_{obs}). For example, k_{obs} of 1.67 h^{-1} and 2.02 h^{-1} were recorded at H_2 pressures of 5 and 7.5 bar (Table 2, entries 3 and 6). Linear relationships were observed from the plot of $\ln [\text{Sty}]_0/[\text{Sty}]_t$ vs time at different H_2 pressures (Fig. S4) to generate a rate order of 0.7 ± 0.1 with respect to H_2 concentration (Fig. 3). This fractional and lower order indicates a complex reaction mechanism with respect to $[H_2]$ and possibly, the formation of a Pd-monohydride species as the active species [25]. The rate law for the hydrogenation reactions of styrene using catalyst 2 can therefore be expressed as given in Eq. (4).

$$\text{Rate} = k[\text{styrene}]^1 [2]^{0.7} [P_{H_2}]^{0.7} \quad (4)$$

3.2.3. Effect of temperature and solvents on styrene hydrogenation kinetics

The effect of temperature on the kinetics of hydrogenation of styrene using catalyst 2 was investigated by comparing the catalytic activities of 2 from 30 °C to 60 °C (Table 3, entries 1–4). The observed rate constants at different temperatures in Table 3 were extracted from the plot of $\ln[\text{styrene}]_0/[\text{styrene}]_t$ vs time (Fig. S5). Expectedly, a significant increase in the rate constant from 1.67 h^{-1} to 6.30 h^{-1} was recorded with an increase in reaction temperature from 30 °C to 60 °C. The overall activation energy (E_a) of the hydrogenation of styrene using 2 was calculated from the Arrhenius plot of $\ln k_{obs}$ vs $1/T$ (Fig. 4a) as $35.61 \pm 1.6 \text{ kJ mol}^{-1}$. This value is comparable to the value of $42.05 \pm 0.01 \text{ kJ mol}^{-1}$ ($10.05 \pm 0.01 \text{ kcal mol}^{-1}$) reported by Pelagatti *et al.* [26] in the hydrogenation reaction of alkenes at 40 °C and are in good agreement with the TOFs of 600 h^{-1} and 580 h^{-1} obtained for

Table 4
Effect of substrate on the catalytic performance of complexes **2** and **6**.^a

Entry	Substrate	K_{obs} (h ⁻¹)		TOF (h ⁻¹) ^b		%Alkanes ^c	
		2	6	2	6	2	6
1	Styrene	1.67 (± 0.01)	2.93 (± 0.01)	368	396	92	99
2	1-hexene	0.69 (± 0.06)	0.97 (± 0.03)	284	312	42	71
3	1-Octene	0.58 (± 0.13)	0.73 (± 0.02)	268	276	40	67
4	1-Nonene	0.56 (± 0.05)	0.62 (± 0.11)	236	248	37	59
5	1-Decene	0.50 (± 0.07)	0.54 (± 0.05)	220	232	33	55
6	Phenyl-acetylene	2.40 (± 0.05)	3.10 (± 0.04)	400	400	100	100
7	1-Hexyne	2.92 (± 0.04)	3.17 (± 0.07)	260	372	59	65
8	1-Octyne	2.29 (± 0.02)	2.91 (± 0.06)	208	356	52	52

^bTOF in mol_{substrate}mol_{catalyst}⁻¹ h⁻¹.

^aConditions: substrate, substrate/catalyst = 600; solvent, toluene; pressure, 5 bar; temperature, 30 °C; time, 1.5 h.

^cSelectivity towards alkane hydrogenation products after 1.5 h.

2 and the Pelagatti catalyst respectively. The Eyring plot in Fig. 4b was used to obtain the enthalpy of activation ($\Delta H^\ddagger = 32.98 \pm 1.9 \text{ kJ mol}^{-1}$) and entropy of activation ($\Delta S^\ddagger = -127.9 \pm 1.9 \text{ J mol}^{-1} \text{ K}^{-1}$). The significance of these thermodynamic parameters is that they support largely homogeneous nature of catalyst **2** as has been previously reported by others [27,28]. Typical heterogeneous catalysts in which the hydrogenation reactions are diffusion controlled display lower values of E_a between 8 kJ mol^{-1} to 17 kJ mol^{-1} [27,28].

We also studied the effects of solvents using toluene, THF, dichloromethane, methanol and DMSO in the hydrogenation reactions of styrene using complex **2** (Table 3, entries 1, 5–8). The order of reactivity was established as follows: DMSO < methanol < THF < toluene. For example, higher catalytic activities were obtained in toluene (k_{obs} of 1.67 h^{-1} , TOF = 368 h^{-1}) than DMSO (k_{obs} of 0.52 h^{-1} , TOF = 183 h^{-1}). This trend is in line with different coordinating

abilities of the solvents; where strongly coordination solvents are known to compete with the alkene substrate, for the active site resulting in diminished activities [29,30]. Consistent with our observations, Unver and Yilmaz recently reported 27% and 63% conversions in DMSO and toluene solvents respectively in the hydrogenation of 1-octene catalyzed by ruthenium complexes [31].

4. Effect of alkene and alkyne substrates on styrene hydrogenation kinetics and selectivity

Complexes **2** and **6** were further used to investigate the hydrogenation reactions of a range of alkene and alkyne substrates: 1-hexene, 1-octene, 1-nonene, 1-decene, phenyl-acetylene, 1-hexyne and 1-octyne. It was observed that the catalytic performance of complexes **2** and **6** were controlled by the nature of the substrate (Tables 4). The initial

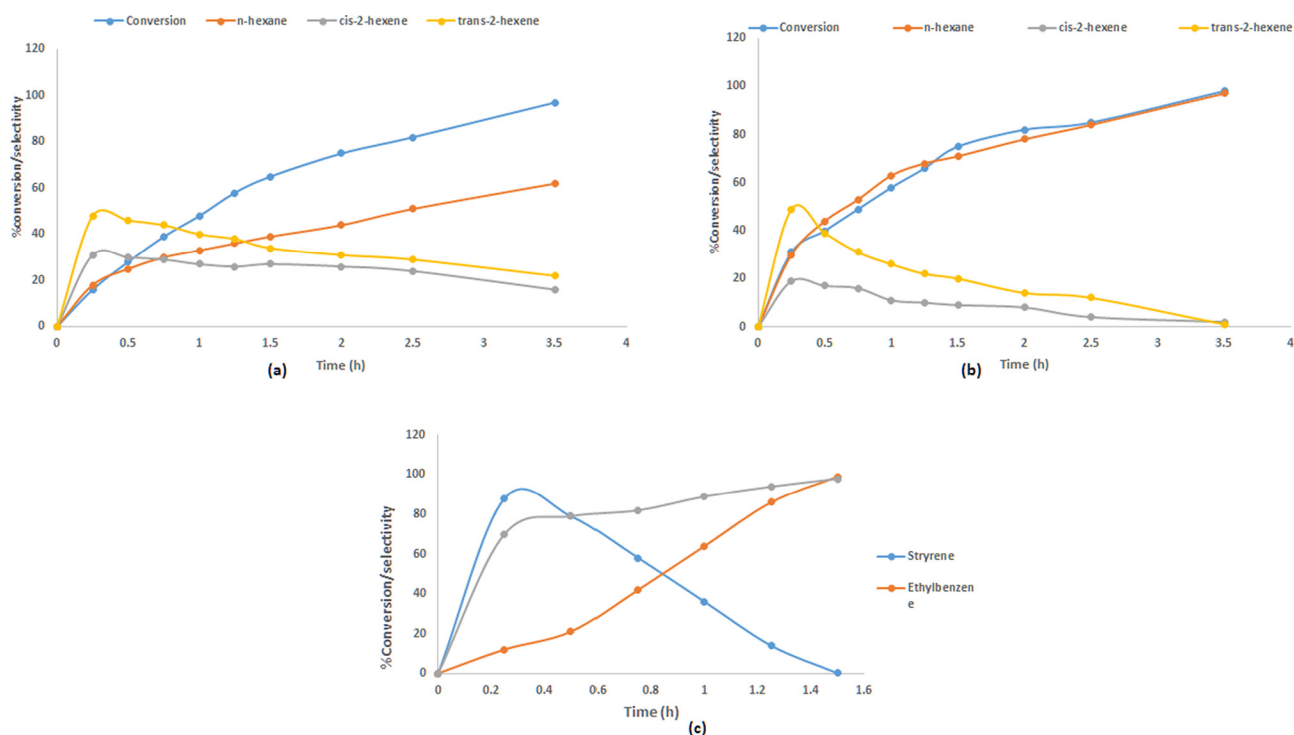
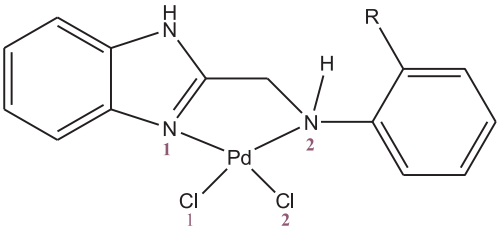


Fig. 5. Product distribution over time in the hydrogenation of (a) 1-hexene and catalyst **2** (b) 1-hexene and catalyst **6** and (c) phenyl-acetylene using catalyst **2**.

Table 5

DFT calculated data for palladium (II) complexes using B3LYP/LANL2DZ level of theory.



R = OCH₃ (1); Br (2); H (3); SH (4)

Parameter	1	2	3	4
LUMO (eV)	−1.87	−1.83	−1.77	−1.81
HOMO (eV)	−7.13	−6.38	−6.75	−6.35
ΔE _{L-H}	5.26	4.55	4.98	4.54
Δε[kcal mol ^{−1}]	121	104	115	105
NBO charges (Pd) 0.326	0.392		0.354	0.358
TOF (h ^{−1}) ^a	296	368	312	344
k _{obs} (h ^{−1})	0.91	1.67	0.98	1.38

^aTOF in mol_{substrate} mol_{catalyst}^{−1} h^{−1}.

rate constants (k_{obs}) of each substrate were determined from the plot of $\ln[\text{substrate}]_0/[\text{substrate}]_t$ vs time (Fig. S6). The results obtained generally showed that alkynes were more reactive compared to the corresponding alkenes [32,33]. For example, k_{obs} of 0.69 h^{−1} and k_{obs} of 2.92 h^{−1} were obtained for 1-hexene and 1-hexyne (Table 4, entries 2

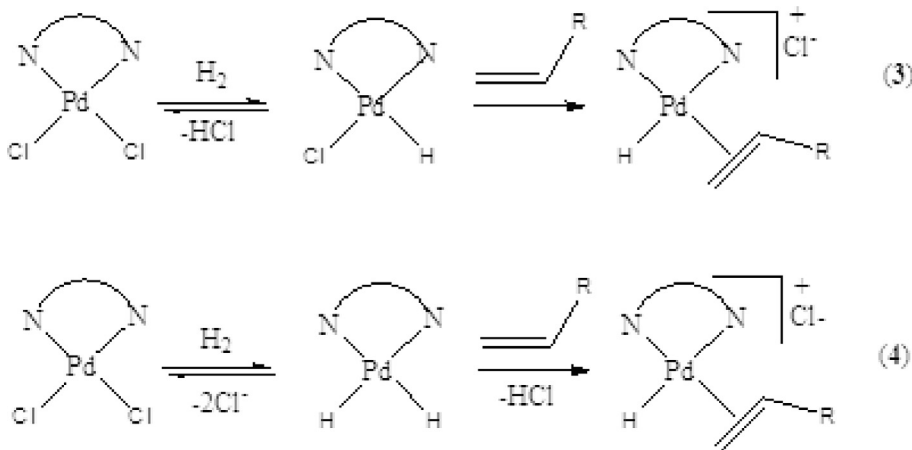
Fig. 5 that catalyst 2 favored isomerization (58% internal isomers) over hydrogenation (42% hexanes), in comparison to catalyst 6 (71% hexanes and 29% internal alkenes). Lower isomerization reactions observed for catalyst 6 can be easily apportioned to the presence of bulkier PPh₃ groups in the metal coordination sphere as has been recently reported by Smarun *et al.* [35].

4.1. Theoretical insights of the hydrogenation reactions of alkenes

Density Functional Theory (DFT) calculations were conducted in order to have an understanding of the effect of the ligand motif and catalyst structure on the catalytic activities of complexes 1–4. The geometries-optimized structures and frontier orbital energy (HOMO and LUMO) maps are summarized in Table 5 and Fig. S7, respectively. The charge on the metal ion was also observed to influence the catalytic activities of complexes 1–4 (Fig. S8). For instance, catalyst 2 carrying a positive charge of 0.392 was more active than catalyst 1, with a charge of 0.326 on the palladium (II) atom. This trend is in agreement with a more facile substrate coordination to an electrophilic palladium atom [36].

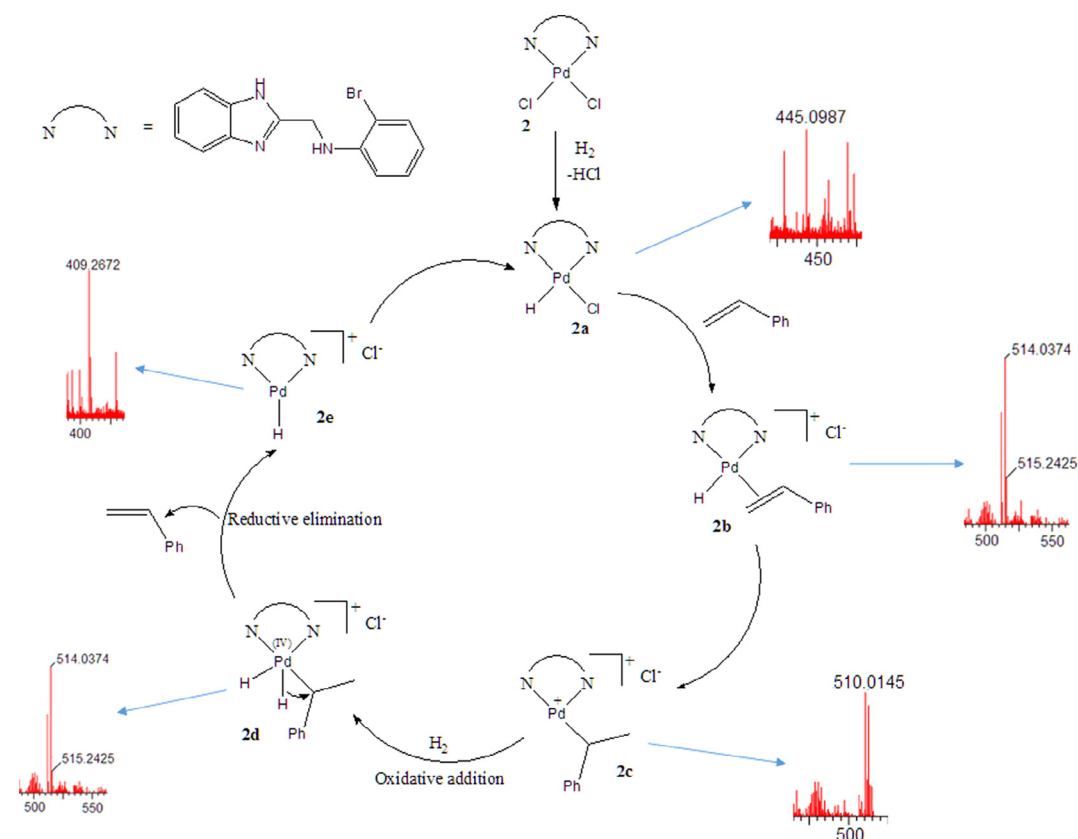
4.2. Proposed mechanism of the hydrogenation of styrene

The dependency of the rate of hydrogenation reactions on styrene, catalyst and hydrogen pressure (Eq. (2)) is consistent with equations (3) and (4). The partial and lower order of reaction with respect to [H₂] of 0.7 ± 0.1 support the formation of a monohydride species as the rate determining step. This points to mechanism (3) as the most probable pathway [37].



and 7). The alkyl chain length had a profound effect on the reactivity of the substrates, in which shorter chains were more reactive. For instance, k_{obs} of 0.97 h^{−1} and 0.54 h^{−1} were observed for 1-hexene and 1-decene respectively (Table 4, entries 2 and 5). The decrease in catalytic activity with alkene chain has been attributed to poor coordinating abilities of higher alkenes to the active metal center [11]. With respect to alkenes, the best catalytic activity for both catalysts 2 and 6 was obtained using styrene to give k_{obs} of 1.67 h^{−1} and 2.93 h^{−1} respectively. This trend has largely been associated with the formation of the more reactive benzylic palladium intermediate, which has a lower energy than alkyl palladium intermediates [34]. The product distribution of terminal alkenes and alkynes was similar to our recent reports [20,21]; where hydrogenation reactions of terminal alkenes were followed by isomerization reactions to give the corresponding internal alkenes, while alkyne hydrogenation reactions occurred in two steps to produce the respective alkenes and alkanes (Fig. 5). It was clear from

In order to fully establish if the pathway given in Eq. (3) is indeed the preferred one, we used ESI-MS (Figure S9) to detect the reaction intermediates (Scheme 1). This was done by sampling of the reaction mixture of complex 2 at various intervals and analysing the aliquots using ES-MS. The mono-hydride intermediate (2a) as observed from MS ($m/z = 445$ amu) is believed to occur via heterolytic cleavage leading to the formation of an HCl by-product [38] pointing to Eq. (3) as the operative mechanism. Coordination of the styrene substrate to 2a affords the Pd-styrene adduct (2b) as deduced from the base peak at $m/z = 514$ amu. A Markovnikov migration of the hydride to the coordinated substrate to form a 14-electron Pd-alkyl species (2c) was established from the m/z signal at 510 amu. Subsequent oxidative addition in the presence of H₂ to give the Pd(IV) dihydride compound (2d) was confirmed from the signal at $m/z = 515$ amu. Hydride migration to give the coordinated alkyl ligand in 2d followed by reductive elimination to produce the monohydride Pd(II) intermediate 2e ($m/$



Scheme 1. Mechanism for the hydrogenation of styrene catalyzed by **2** as established from ESI-MS, m/z corresponds to the cationic palladium fragments.

$z = 409$) and elimination of the ethylbenzene product was also confirmed. Finally, it is believed that regeneration of the active hydride species **2a** ($m/z = 450$) completes the catalytic cycle. Attempts to confirm the formation of the Pd-hydride intermediates using ^1H NMR spectroscopy has not been successful even at elevated temperatures (Fig. S10). We did not observe any signal associated with the Pd-H (around -0.5 ppm) and this may be due to low pressures (atmospheric) employed in the NMR studies as opposed to higher pressures of 5–30 bar used in the catalytic experiments.

5. Conclusions

In summary, we have established that neutral and cationic palladium (II) complexes anchored on (benzoimidazol-2-ylmethyl)amine ligands form active catalysts for the hydrogenation reactions of alkenes and alkynes in which isomerization of terminal alkenes also occur. The electrophilicity of the palladium atom in the complexes atom as supported by DFT calculations, enhanced the reactivity of the respective catalysts. Longer chain alkenes showed diminished reactivity while alkynes were generally more reactive compared to the correspond alkenes. Kinetics, thermodynamics and mercury drop experiments point to largely homogeneous systems. A mechanistic pathway involving the formation of a palladium monohydride intermediate as the active species was established from mass spectrometry.

Acknowledgement

The authors are highly indebted to the National Research Foundation (NRF-South Africa) for proving PhD scholarship to the first author. The NRF-DST Centre of Excellence in Catalysis, (c*change, OLE10.3-UKZN) and competitive program for rated researchers (grant number: CPRR 98938) are also appreciated for their financial support.

Conflict of interest statement

The authors declare no conflict of interests in this manuscript with any other third party, individual or organization.

Appendix A. Supplementary data

Supplementary data associated with this article can be found, in the online version, at <https://doi.org/10.1016/j.ica.2018.08.004>.

Reference

- [1] K.A. Vallianatou, D.J. Frank, G. Antonopoulou, S. Georgakopoulos, E. Siapi, M. Zervou, I.D. Kostas, *Tetrahedron Lett.* 54 (2013) 397–401.
- [2] H.E. Hoelscher, W.G. Poynter, E. Weger, *Chem. Rev.* 54 (1954) 575–592.
- [3] C. Bianchini, A. Meli, M. Peruzzini, P. Frediani, C. Bohanna, M.A. Esteruelas, L.A. Oro, *Organometallics* 11 (1992) 138–145.
- [4] D. Schleyer, H.G. Niessen, J. Bargon, *New J. Chem.* (2001) 423–426.
- [5] J. Navarro, M. Sagi, E. Sola, F.J. Lahoz, I.T. Dobrinovitch, A. Katho, F. Joo, L.A. Oro, *Adv. Synth. Catal.* 345 (2003) 280–288.
- [6] F. Nerozzi, *Platin. Met. Rev.* 56 (2012) 236–241.
- [7] M. Irfan, T.N. Glasnov, C.O. Kappe, *ChemSusChem* 4 (2011) 300–316.
- [8] E. Negishi, *Handbook of Organopalladium Chemistry for Organic Synthesis*, Wiley & Sons, New York 1 (2002) 229–247.
- [9] A. Bacchi, M. Carcelli, M. Costa, A. Leporati, E. Leporati, P. Pelagatti, C. Pelizzi, G. Pelizzi, *J. Organomet. Chem.* 535 (1997) 107–120.
- [10] D. Drago, P.S. Pregosin, *Organometallics* 21 (2002) 1208–1215.
- [11] P.W.N.M. Leeuwen, J.C. Chadwick, *Homogeneous catalysts: activity-stability-deactivation*, Wiley-VCH Verlag, 2011.
- [12] M.W. van Laren, M.A. Duin, C. Klerk, M. Naglia, D. Rogolino, P. Pelagatti, A. Bacchi, C. Pelizzi, C.J. Elsevier, *Organometallics* 21 (2002) 1546–1553.
- [13] M.W. van Laren, C.J. Elsevier, *Angew. Chemie Int. Ed.* 38 (1999) 3715–3717.
- [14] T.A. Tshabalala, S.O. Ojwach, M.A. Akerman, *J. Mol. Catal. A Chem.* 406 (2015) 178–184.
- [15] N.W. Attandoh, S.O. Ojwach, O.Q. Munro, *Eur. J. Inorg. Chem.* 2014 (2014) 3053–3064.
- [16] M. J. T. Frisch, G. W. Trucks, H. B. Schlegel, G. E. Scuseria, M. A. Robb, J. R. Cheeseman, G. Scalmani, V. Barone, B. Mennucci, G. A. Petersson, H. Nakatsuji, M. Caricato, X. Li, H. P. Hratchian, A. F. Izmaylov, J. Bloino, G. Zheng, J. L.

- Sonnenberg, M. Hada, M. Ehara, K. Toyota, R. Fukuda, J. Hasegawa, M. Ishida, T. Nakajima, Y. Honda, O. Kitao, H. Nakai, T. Vreven, J. A. Montgomery Jr., J. E. Peralta, F. Ogliaro, M. Bearpark, J. J. Heyd, E. Brothers, K. N. Kudin, V. N. Staroverov, R. Kobayashi, J. Normand, K. Raghavachari, A. Rendell, J. C. Burant, S. S. Iyengar, J. Tomasi, M. Cossi, N. Rega, J. M. Millam, M. Klene, J. E. Knox, J. B. Cross, V. Bakken, C. Adamo, J. Jaramillo, R. Gomperts, R. E. Stratmann, O. Yazyev, A. J. Austin, R. Cammi, C. Pomelli, J. W. Ochterski, R. L. Martin, K. Morokuma, V. G. Zakrzewski, G. A. Voth, P. Salvador, J. J. Dannenberg, S. Dapprich, A. D. Daniels, O. Farkas, J. B. Foresman, J. V. Ortiz, J. Cioslowski, D. J. Fox, GAUSSIAN 09 (Revision A.1), Gaussian, Inc., Wallingford, CT, 2009.
- [17] R.R. Schrock, J.A. Osborn, *J. Am. Chem. Soc.* 98 (1976) 2134–2143.
- [18] J.A. Osborn, F.H. Jardine, J.F. Young, G. Wilkinson, J., *Chem. Soc. A Inorganic Phys. Theor.* (1966) 1711.
- [19] V. Goudy, A. Jaoul, M. Cordier, C. Clavaguéra, G. Nocton, *J. Am. Chem. Soc.* 139 (2017) 10633–10636.
- [20] S.O. Ojwach, A.O. Ogwenio, M.P. Akerman, *Catal. Sci. Technol.* 6 (2016) 5069–5078.
- [21] S.O. Ojwach, A.O. Ogwenio, *Transit. Met. Chem.* 41 (2016) 539–546.
- [22] J.A. Widegren, R.G. Finke, *J. Mol. Catal. A Chem.* 198 (2003) 317–341.
- [23] V.P. Ananikov, I.P. Beletskaya, *Organometallics* 31 (2012) 1595–1604.
- [24] A.M. Kluwer, T.S. Koblenz, T.T. Jonischkeit, K. Woelk, C.J. Elsevier, *J. Am. Chem. Soc.* 127 (2005) 15470–15480.
- [25] P.J. Rheinlander, J. Herranz, J. Durst, H.A. Gasteiger, *J. Electrochem. Soc.* 161 (2014) F1448–F1457.
- [26] P. Pelagatti, A. Bacchi, M. Carcelli, M. Costa, A. Fochi, P. Ghidini, E. Leporati, M. Masi, C. Pelizzi, G. Pelizzi, *J. Organomet. Chem.* 583 (1999) 94–105.
- [27] F. Joó, L. Nádasdi, A.C. Béneyei, D.J. Darensbourg, *J. Organomet. Chem.* 512 (1996) 45–50.
- [28] E. Gonzo, M. Boudart, *J. Catal.* 52 (1978) 462–471.
- [29] P.J. Dyson, P.G. Jessop, *Catal. Sci. Technol.* 6 (2016) 3302–3316.
- [30] F. Yilmaz, A. Mutlu, H. Ünver, M. Kurta, I. Kani, *J. Supercrit. Fluids* 54 (2010) 202–209.
- [31] H. Ünver, F. Yilmaz, *Catalysts* 6 (2016) 147.
- [32] D. Teschner, J. Borsodi, A. Wootsch, Z. Revay, M. Havecker, A. Knop-Gericke, S. D. Jackson, R. Schlögl, *Science* (80-.), 2008, 320, 86–89.
- [33] H. Yoshida, T. Zama, S. Fujita, J. Panpranot, M. Arai, *RSC Adv.* 4 (2014) 24922.
- [34] P.K. Santra, P. Sagar, *J. Mol. Catal. A Chem.* 197 (2003) 37–50.
- [35] A.V. Smarun, W. Shahreel, S. Pramono, S.Y. Koo, L.Y. Tan, R. Ganguly, D. Vidović, *J. Organomet. Chem.* 834 (2017) 1–9.
- [36] T. Sperger, I.A. Sanhueza, I. Kalvet, F. Schoenebeck, *Chem. Rev.* 115 (2015) 9532–9586.
- [37] K.C. Dewhirst, W. Keim, C.A. Reilly, *Inorg. Chem.* 7 (1968) 546–551.
- [38] S.P. Smidt, N. Zimmermann, M. Studer, A. Pfaltz, *Chem. A Eur. J.* 10 (2004) 4685–4693.